

Polarization reversal of electron cyclotron waves creating plasma-potential structures in laboratory plasmas

Kazunori Takahashi^{1,2}, Toshiro Kaneko¹, Rikizo Hatakeyama¹

¹Department of Electronic Engineering, Tohoku University, Sendai 980-8579, Japan
kazunori@iwate-u.ac.jp, kaneko@ecei.tohoku.ac.jp, hatake@ecei.tohoku.ac.jp

²Department of Electrical and Electronic Engineering, Iwate University, Morioka 020-8551, Japan

Abstract

Selectively launched electromagnetic waves for azimuthal mode number $m=0$, and $m=\pm 1$ modes are investigated around an electron cyclotron resonance (ECR) region in inhomogeneously magnetized plasmas. A left-hand polarized wave for $m=0$ is unexpectedly absorbed at the ECR point as a result of a polarization reversal in the axial direction. For $m=\pm 1$, the polarization reversal occurs along the radial axis. Moreover, high-power $m=\pm 1$ waves can selectively form electric double layers at the center and peripheral areas with the potential jump corresponding to an ion flow energy; the selective formation is due to absorption profiles resulting from the polarization reversal.

1. Introduction

It is crucial to investigate propagation and absorption of electromagnetic waves with electron cyclotron resonance (ECR) frequencies in inhomogeneously magnetized plasmas from the viewpoint of magnetospheric physics and laboratory applications. In the field of magnetospheric physics, electron acceleration inside the Earth's magnetosphere is required to explain increase in the relativistic electrons (> 1 MeV) flux during the geomagnetic storms. The resonant scattering process via electromagnetic whistler mode waves has been recognized as the strong candidate for the acceleration mechanism of the electrons [1]. Moreover, ECR heating has also been considered as the origin of diffuse aurora [2]. As mentioned above, the characteristics of the waves in the range of ECR frequencies would be playing important roles in the unsolved phenomena in space. On the other hand, ECR is effective for producing plasmas with high density, large diameter, and a uniform density profile in the field of processing plasmas. It is obvious that the wave propagation and absorption determine the heating efficiency and characteristics of the produced plasmas.

Concerning the linear wave propagation in the laboratory experiments, there were a few questions that the absorption of the left-hand polarized wave launched by a helical antenna in a magnetic beach is unexpectedly observed [3], that the $m=-1$ mode wave can create high-density plasmas by ECR [4], although the linear wave propagations has been considered to be well understood.

In this paper, we show the experimental evidence of the polarization reversal in the axial direction in launching a left-hand polarized wave by the helical antenna, where the polarization is reversed from left to right handed in front of the ECR point. The polarization reversal causes the unexpected ECR absorption of the left-hand polarized wave. In this case, we identified the azimuthal mode number m of the wave as $m = 0$. In addition, $m = \pm 1$ mode waves are also investigated in these experiments; the polarization reversal not in the axial direction but in the radial direction is observed, i.e., a wave polarization for $m=+1$ ($m=-1$) mode is right (left) handed around the center and left (right) handed in the peripheral area. The polarization profile dominates the wave-absorption profile and the ECR heating profile in the cross section of the plasma column. Moreover, plasma-potential structures created by the high-power $m = \pm 1$ mode waves are revealed now, where a field-aligned potential jump, i.e., an electric double layer is formed at the center and peripheral areas for $m=+1$ and -1 , respectively.

2. Linear Dispersion Analysis in Bounded Plasmas

We consider an azimuthally and radially uniform plasma column. A dispersion relation in cold plasmas is derived from the Maxwell equations as

$$(\gamma^2 + \kappa_2^2 + \gamma k_\perp^2)\kappa_3 + k_\perp^2[\kappa_1(\gamma + k_\perp^2) - \kappa_1^2] = 0, \quad (1)$$

where $\gamma \equiv k_\parallel^2 - \kappa_1$, and k_\parallel and k_\perp are the wave numbers parallel and perpendicular to a static magnetic field \mathbf{B} in the z -direction, respectively. κ_1 , κ_2 , and κ_3 are the components of the dielectric tensor following Swanson notation [5]. The

electric fields are assumed to propagate in the z -direction, therefore, wave fields with azimuthal mode number m can be represented by $\mathbf{E}(r)\exp[i(k_{\parallel}z + m\theta - \omega t)]$, where the components of the electric-field vector are represented by the Bessel function of order m . In a bounded plasma with a diameter comparable to the wavelength of the electromagnetic wave, the perpendicular wavenumber k_{\perp} is determined by radial boundary conditions. The detailed analysis is described in Refs. [6,7].

The wave polarization plays important roles in the cyclotron resonance phenomena. The above dispersion relation and electric-field components derive a polarization index S as $S \equiv |E_r + i E_{\theta}| / |E_r - i E_{\theta}|$. Here, $0 < S < 1$ and $1 < S < \infty$ represent right- and left-handed polarization, respectively. The wave polarization can become both right and left handed, and depends on the plasma parameters such as electron density and magnetic-field strength.

3. Experiments on $m = 0$ mode left-hand polarized wave

Top and bottom figures in Fig. 1 shows the experimental setup for the propagation of the $m=0$ mode left-hand polarized wave, and the external magnetic-field configuration. The machine has a 450-cm-long 20.8-cm-diam earthed vacuum chamber. A coaxial bounded plasma is produced by a dc discharge between an oxide cathode and a mesh anode in low pressure argon gas (90 mPa). A clear boundary between the plasma and the vacuum area is created using a limiter (plasma radius is 3 cm). Langmuir probe measurements shows a uniform density profile of about $n_e = 9 \times 10^{10} \text{ cm}^{-3}$. External magnetic-field configuration is inhomogeneous as shown in the bottom of Fig. 1. A microwave (frequency $\omega / 2\pi = 6 \text{ GHz}$, power $P_{\text{in}} = 150 \text{ mW}$) is selectively launched in the high magnetic-field side ($z = 0 \text{ cm}$) as a left-hand polarized wave (LHPW) by a helical antenna. The each component of the wave electric field (E_x, E_y, E_z) is detected through axially and radially movable balanced dipole antennas.

Figure 2(a) shows the interferometric wave patterns of E_x (dashed line) and E_y (solid line), which indicate the damping of the launched wave near the ECR point in spite of the selective launch of the LHPW. It is to be noted that the wave patterns include both the long (LW) and the short (SW) wavelength components. The LW and SW are decomposed from the wave patterns in Fig. 2(a) by Fourier analysis and presented in Fig. 2(b). Fig. 2(b) shows that the LW damps and the SW grows around $z = 60 \text{ cm}$ and that the wave patterns of E_x in the LW and the SW are shifted to the left and to the right of E_y , respectively. From the phase differences, the LW and the SW are identified as a LHPW and a right-hand polarized wave (RHPW). Therefore, the patterns in Fig. 2 evidences that the LHPW damps and the RHPW grows around $z = 60 \text{ cm}$; a polarization is reversed from left to right handed in the axial direction. As a result of the polarization reversal in the axial direction, the launched LHPW is absorbed near the ECR point, because the polarization has already changed into right handed at the ECR point.

Figure 3(a) shows the calculated dispersion relation (solid line) together with experimental dispersion of the LHPW (LW in Fig. 2(b): closed circle) and the RHPW (SW in Fig. 2(b): open square), where ω_{ce} is the local electron cyclotron frequency. The calculated dispersion curve of the slow wave is in good agreement with the experimental ones. The polarization index S is also plotted in Fig. 3(b) for theoretical verification of the polarization reversal in the axial direction. The value of S is

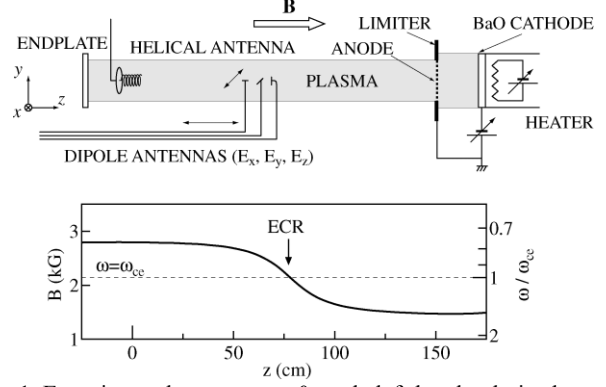


Fig. 1. Experimental setup on $m=0$ mode left-hand polarized wave.

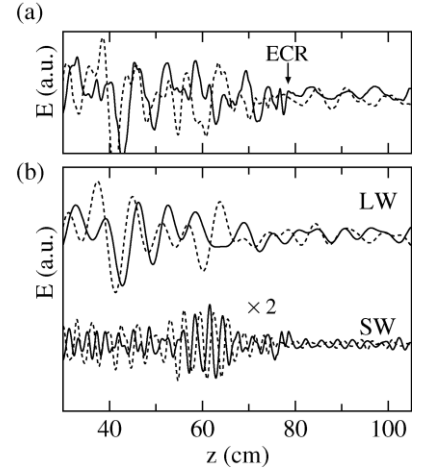


Fig. 2. (a) Interferometric wave patterns of E_x (dashed line) and E_y (solid line). (b) LW and SW components included in the wave patterns of Fig. 2(a).

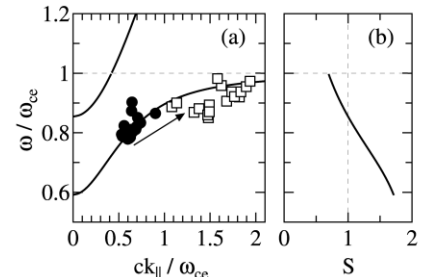


Fig. 3. (a) Calculated dispersion relation (solid line) together with experimental dispersion of the LHPW [LW in Fig. 2(b)] and the RHPW [SW in Fig. 2(b)]. (b) Calculated polarization index S .

larger than unity in the range of $\omega/\omega_{ce} < 0.85$, i.e., the polarization is left handed. As the wave approaches the ECR point ($\omega/\omega_{ce} = 1$), S becomes smaller than unity. Therefore, it is theoretically explained that the polarization is reversed along the axis. The detailed experimental results have already been reported in Refs. [6-8].

4. Experiments on $m = \pm 1$ mode waves

Figure 4 shows (a) the experimental setup on $m = \pm 1$ mode waves investigation and (b) the external magnetic-field configuration of types (I) and (II). A plasma source for controlling the ion flow energy under low argon gas pressure (10 mPa) is set at the low field side. The basic behavior of this source has already reported by authors [9]. In this experiments, an anode voltage deciding the ion flow energy is fixed at $V_a = 15$ V. The plasma radius is limited about 3 cm by a limiter located at the position of the anode. Microwave ($\omega/2\pi = 6$ GHz) with $m = \pm 1$ modes are selectively launched from the high magnetic-field side using a horn antenna with a dielectric polarizer. It is confirmed an axial ratio of the circularly polarized wave radiated from the antenna is about 1.1. The ECR point of 6 GHz microwave are $z = 26$ and 45.5 cm under configurations (I) and (II), respectively. Here, $z = 0$ and each axis (x, y, z) is defined on the basis of the axial center of the machine and as indicated at the upper right of Fig. 4(a). Spatial profiles of plasma parameters are measured by two single-tipped Langmuir probes, which are movable in x - z plane at $y = 0$ cm and in x - y plane at $z = 26$ cm, respectively. Electric fields $E_x, E_y,$ and E_z of the microwaves are measured using movable dipole antennas, where spatial profiles of wave phase are directly obtained using a network analyzer; the phase difference between E_x and E_y allow us to identify the wave polarization.

Figure 5 shows x profiles of the theoretical polarization index S (solid line) and the experimentally obtained phase difference $\Delta\theta$ (open circle) between E_x and E_y of the waves for (a) $m = +1$ and (b) $m = -1$ modes at $z = 15$ cm under configuration (I), where the right- and left-handed polarizations are represented by $-180^\circ < \Delta\theta < 0^\circ$ and $0^\circ < \Delta\theta < 180^\circ$, respectively. In Fig. 5, the gray and white parts show the right- and left-handed polarizations for both $\Delta\theta$ and S . It is found in Fig. 5(a) the polarization for $m = +1$ is right handed around the center area and left handed around the peripheral area, i.e., the polarization is reversed along the radial axis in both the theoretical analysis and the experimental observations. In contrast, the left- and right-handed polarizations are observed around the center and peripheral areas for the case of $m = -1$ as indicated in Fig. 5(b). Originating from these polarization profile, we could observe in the experiments and confirm in the simulation (not shown here) that the waves are absorbed around the center and peripheral areas for $m = +1$ and -1 modes, respectively. Thus, it is clarified that the waves are absorbed around the area where the polarization is right handed. In the next section, we report a plasma-potential structures created by these wave-absorption characteristics.

5. Experiments on plasma-structure formation by high-power $m = \pm 1$ mode waves

In this section, the plasma-potential-structure created by the high-power $m = \pm 1$ mode electron cyclotron waves, whose propagation characteristics has already reported in the previous section. The experimental setup is basically same as Fig. 4, where a klystron is used for the amplifier of the microwave ($\omega/2\pi = 6$ GHz, $P_{in} = 50$ W).

Figure 6 gives two-dimensional profiles of the plasma potential ϕ_p in the x - z plane and the x - y plane for (a)(b) $P_{in} = 0$ W, (c)(d) $P_{in} = 50$ W with $m = +1$ mode, and (e)(f) $P_{in} = 50$ W with $m = -1$ mode, where the anode potential is fixed at $V_a = 15$ V. ϕ_p for $P_{in} = 0$ W is homogeneous as shown in Figs. 6(a) and 6(b). In the case of $m = +1$ mode shown in Figs. 6(c) and 6(d), an electric double layer (DL), i.e., the field-aligned potential jump, is found to be formed around

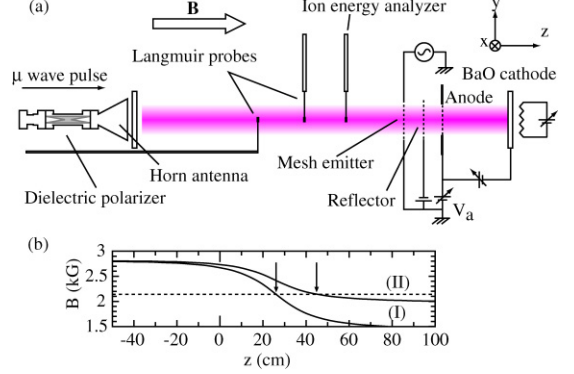


Fig. 4. (a) Experimental setup on $m = \pm 1$ mode waves. (b) Magnetic-field configuration (I) and (II).

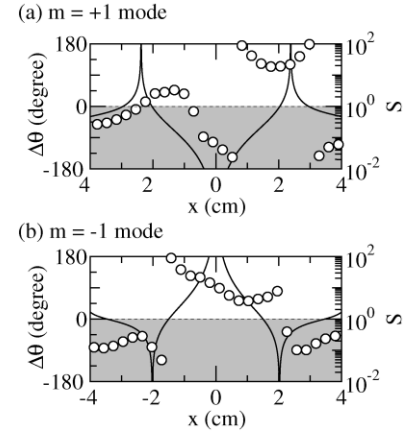


Fig. 5. x profiles of the theoretical polarization index S (solid line) and the experimentally obtained phase difference $\Delta\theta$ (open circle) between E_x and E_y of the waves for (a) $m = +1$ and (b) $m = -1$ modes at $z = 15$ cm under configuration (I).

the center area of the cross section of the plasma column. Here, we mention the potential height corresponds to the field-aligned ion flow energy, and its detailed physics are described in Ref. [10]. In the case of $m = -1$ mode, on the other hand, the DL is formed around the peripheral area as presented in Figs. 6(e) and 6(f). The selective formation of the DL in the center and peripheral areas are originating from the ECR heating profile, the wave-absorption profile, and the polarization profile as reported in Sec. 4.

6. Conclusion

In summary, selectively launched electromagnetic waves for azimuthal mode number $m=0$, and $m=\pm 1$ modes waves in laboratory plasmas are investigated around an electron cyclotron resonance (ECR) region in inhomogeneously magnetized plasmas.

A left-hand polarized wave for $m=0$, which is considered not to be related to ECR absorption, is unexpectedly absorbed at the ECR point as a result of a polarization reversal in the axial direction. For $m=\pm 1$, the polarization reversal occurs along the radial axis. These phenomena, i.e., polarization reversal in the axial and radial direction are well explained by the dispersion analysis in bounded plasmas, where the wavenumber perpendicular to the magnetic-field lines are fixed by the radial boundary condition.

Moreover, plasma-potential structures created by high-power $m=\pm 1$ waves are also investigated. In this experiment, an electric double layer (DL), i.e., the potential jump along the field lines, is formed near the ECR point in the center and peripheral areas for the case of $m = +1$ and -1 modes, respectively. The propagation and absorption characteristics, especially polarization of the waves, are playing an important role in the formation of the plasma structures. We hope these results would be useful for the studies on the plasma-structure formation in space.

7. References

1. Y. Katoh and Y. Omura, "Acceleration of relativistic electrons due to resonant scattering by whistler mode waves generated by temperature anisotropy in the inner magnetosphere", *J. Geophys. Res.*, **109**, 2004, pp. A12214-1-9.
2. R. B. Horne, R. M. Thorne, N. P. Meredith, and R. R. Anderson, "Diffuse auroral electron scattering by electron cyclotron harmonic and whistler mode waves during an isolated substorm", *J. Geophys. Res.*, **108**, 2003, pp. SMP14-1-14.
3. T. Kaneko, H. Murai, R. Hatakeyama, and N. Sato, "Experimental evidence for spatial damping of left-hand circularly polarized waves in an electron cyclotron resonance region", *Phys. Plasmas*, **8**, 2001, pp. 1455-1458.
4. A. Ganguli, M. K. Akhtar, R. D. Tarey, and R. K. Jarwal, "Absorption of left-polarized microwaves in electron cyclotron resonance plasmas", *Phys. Lett. A*, **250**, (1998), pp. 137-143.
5. D. G. Swanson, *Plasma Waves 2nd edition*, Institute of Physics, Bristol and Philadelphia, 2003.
6. K. Takahashi, T. Kaneko, and R. Hatakeyama, "Effects of polarization reversal on localized-absorption characteristics of electron cyclotron wave in bounded plasmas", *Phys. Plasmas*, **12**, 2005, pp. 102107-1-7.
7. K. Takahashi, T. Kaneko, and R. Hatakeyama, "Absorption and penetration of left-hand polarized waves related to polarization reversal causing electron cyclotron resonance", *Phys. Rev. E*, **74**, 2007, pp. 016405-1-7.
8. K. Takahashi, T. Kaneko, and R. Hatakeyama, "Polarization-reversal-induced damping of left-hand polarized wave on electron cyclotron resonance", *Phys. Rev. Lett.*, **94**, 2005, pp. 215001-1-4.
9. K. Takahashi, T. Kaneko, and R. Hatakeyama, "Simultaneous control of ion flow energy and electron temperature in magnetized plasmas", *Appl. Phys. Lett.*, **88**, 2006, pp. 111503-1-3.
10. K. Takahashi, T. Kaneko, and R. Hatakeyama, "Field-aligned and transverse plasma-potential structures induced by electron cyclotron waves", *Appl. Phys. Lett.*, **91**, 2007, pp. 261502-1-3.

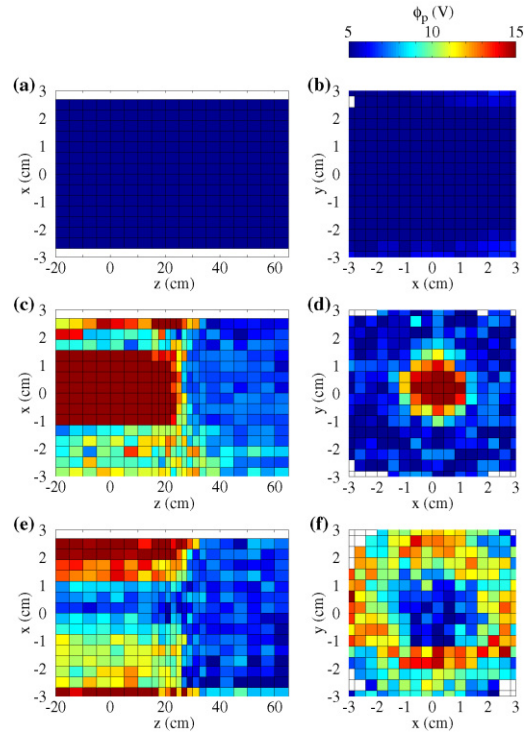


Fig. 6. x - z and x - y profiles of the plasma potential ϕ_p for (a)(b) $P_{in} = 0$ W, (c)(d) $P_{in} = 50$ W with $m = +1$ mode, and (e)(f) $P_{in} = 50$ W with $m = -1$ mode, where the anode potential is fixed at $V_a = 15$ V. (a), (c), and (e) are measured at $y = 0$ cm under configuration (I), while (b), (d), and (f) are obtained at $z = 26$ cm under configuration (II).